CrystEngComm

Accepted Manuscript

ROYAL SOCIETY OF CHEMISTRY

www.rsc.org/crystengcomm

A Polymorph of the 6,13-Dichloropentacene Organic semiconductor: Crystal Structure, Semiconductor Measurements and Band Structure Calculations

Peggy V. Hatcher,[a] Joseph H. Reibenspies,[b] Robert C. Haddon,[c] Dawen Li,[d] Neoro Lopez,[a] Xiaoliu Chi[a*]

[a]Department of Chemistry, Texas A&M University – Kingsville, Kingsville, TX 78363
[b]Department of Chemistry, Texas A&M University, College Station, TX 77842-3012
[c]Departments of Chemistry and Chemical & Environmental Engineering, University of California, Riverside, CA 92521
[d]Department of Electrical and Computer Engineering & Center for Materials for Information Technology, The University of Alabama Tuscaloosa, AL 35487

[*]Email: kfxc000@tamuk.edu

Abstract

Polymorphism is an important issue for the application of organic semiconductors in field-effect transistors due to the dependence of device performance on crystal packing. Recently an organic semiconductor, 6,13-dichloropentacene (DCP), was shown to give a field-effect mobility as high as 9 cm^2/Vs when crystallized in the form of microribbons obtained by physical vapor transport (PVT), in contrast with the much lower mobilities found in crystals grown from solution. In the present manuscript we show that the crystals grown in the vapor phase are a polymorph of the structure reported for the crystals grown from solution. Both polymorphs show a π-stacking motif but differ in the interplanar distances and the displacement of the molecules along the long axes of the molecules. The DCP PVT structure compares favorably to that of rubrene, but DCP shows a much lower mobility. Band structure calculations show that the rubrene crystal exhibits greater band dispersion than DCP even though the long-axis displacement in rubrene is much greater. We conclude that the transport properties cannot be inferred simply by the magnitude of the intrastack long-axis displacement, but requires a consideration of the relative location of the HOMO/LUMO coefficients of the neighboring molecules in the stack.

Keywords: Polymorph, Organic semiconductor, 6,13-dichloropentacene, Organic Field effect Transistor, Crystal Structure, rubrene, band structure

Introduction

Organic semiconductors have been extensively studied in recently years for flexible and low cost electronic applications.[1-5] To realize such applications, however, organic semiconductors have to be soluble and stable with reasonably high charge-carrier mobility. In theory, high mobility can be achieved only when organic molecules strongly interact through intermolecular orbital overlap, and the overlap can be maximized when planar conjugated molecules adopt a cofacial π-stacking arrangement.[6-9] Many efforts have been made to tune organic molecules in order to realize a π-stacking arrangement and hence high mobility.[8,10-12] The importance of molecular ordering, particularly the existence of π-stacking, to high charge-carrier mobility have been demonstrated elegantly in a number of systems,[13,14] such as tetrathiafulvalene derivatives[15] and tetracene derivatives.[16]

In addition to chemical modification of the structure of organic semiconductors, polymorphism is another important issue that affects molecular ordering and hence mobility.[4] In pentacene, for instance, there are at least 4 polymorphs with different electronic structures.[8,17,18] Rubrene has been one of the most extensively studies organic semiconductor for single crystal field-effect transistor study with room temperature mobility of over 20 cm2/Vs.[19,20] Recent studies show that several polymorphs can be obtained by solution crystallization,[21] and two polymorphs were successfully tested in single crystal field effect transistor studies in which it was found that the mobility of the orthorhombic phase was an order of magnitude higher than the triclinic phase.[22] Polymorphism has also studied in other organic semiconductors, where polymorphs with stronger electronic band dispersions give higher mobility.[23] It is therefore important to be aware of and to be able to control of polymorphism if organic semiconductors are to be used for commercial applications.[24]

Recently, Li et al. reported the synthesis and transistor properties of a halogenated pentacene derivative, 6,13-dichloropentacene (**2**, Figure 1).[25,26] Not surprisingly, with electron withdrawing group attached to the pentacene backbone, this compound is more stable and soluble compared with the parent pentacene molecule, and therefore holds promise for device applications. The thin film field effect mobility reaches 0.2 cm^2/Vs, which is comparable with the value obtained from microribbons grown by solution processing. On the other hand, the crystalline ribbons grown by the physical vapor transport (PVT) method displayed a high mobility - up to 9 cm^2/Vs. This high mobility was attributed to the π-stacking arrangement found in the crystal structure (inferred on the basis of the solution grown crystals). However, the crystal structure was reported only for the crystals grown from solution phase, and the structures of the thin film and the crystalline ribbons were taken to be identical to the solution grown crystals from the XRD pattern and by theoretical calculations. It was concluded that the condition of device fabrication has little effect on the structure of DCP, which is important for the potential application of this compound.[26]

We successfully crystallized DCP by the PVT method and obtained the crystal structure and we found that the crystals grown by the PVT method are a polymorph of the solution grown crystals and in the present manuscript we report the synthesis, crystal structure and transistor properties of this polymorph, together with electronic band structure calculations which account for the variations in mobility.

Experimental

General

All reagents were purchased from Aldrich and used as received. Solvent N,N-Dimethylformamide (DMF) was purged for 30 minutes with nitrogen prior to reactions. ^1H NMR spectra was recorded on an Bruker Avance 300 Spectrometer (300-MHz); Mass Spectra were obtained using Voyager STR matrix-assisted laser desorption time-of-flight mass spectrometer (MALDI-TOFMS).

Synthesis

The 6,6,13,13-Tetrachloro-6,13-dihydropentacene: Under nitrogen, phosphorus oxychloride (200.0 mL) is slowly added by dropping funnel to a mixture of phosphorus pentachloride (72 g, 0.34 mol) and 6,13-pentacenequinone (10.5g, 0.034 mol) in a flame-dried round-bottom flask, and the mixture is heated to 130°C for 3 hours. The beige precipitate is collected by filtration and washed with glacial acetic acid and hexane to give a pale yellow solid (80% yield), and the crude product was used without further purification.

6,13-Dichloropentacene: A mixture of NaI (2.2 g, 0.0015 mol) and 6,6,13,13-tetrachloro-6,13-dihydropentacene (15 g , 0.034 mol) in 200 mL of DMF was reflux under nitrogen for 30 minutes without light. After cooling, the precipitate was filtered through a fritted glass filter and washed with ethanol, water and acetone to give dark purple crystalline solid (86% yield). Mp >330^{o}C (decompose; cf. ref 24: mp 298-300^{o}C). NMR (300 MHz, d-chloroform): δ 9.23 (s,4H), 8.05-8.09(m, 4H), 7.44-7.48 (m, 4H). m/z(MALDI, DCTB matrix): 346.333 (M+).

Single crystal growth and characterization

Single crystals for both X- ray and electronic transport measurements were grown by horizontal physical vapor phase transport (PVT) in a stream of high purity argon using a modified apparatus previously described by Laudise et al.[27] Here, two glass tubes of different diameters were used, with the outer tube wrapped with two rope heaters defining source zone and crystal growth zone, respectively. A glass tube of smaller diameter served as the sample container. The source temperature was held at 260 ^{o}C, and the argon flow rate was 19 ml/min. A typical needle-like crystal showed dimensions of 5–12 mm in length, 0.1–0.75mm in width and 0.05-0.1mm in thickness.

A single crystal was analyzed using a BRUKER GADDS X-ray (three-circle) diffractometer, using a Cu sealed X-ray tube (Kα = 1.5418 Å with a potential of 40 kV and a current of 40 mA) fitted with a graphite monochromator in the parallel mode (175

mm collimator with 0.5 mm pinholes). Employing Olex2,[28] the structure was solved with the ShelXT[29] structure solution program using Direct Methods and refined with the ShelXL[30] refinement package using Least Squares minimization.

Band Structure Calculations

The band structure calculations made use of a modified version of the extended Huckel theory (EHT) band structure program originally supplied by M.-H. Whangbo. The parameter set is chosen to provide a reasonably consistent picture of bonding in heterocyclic organic compounds. [9,31,32]

Fabrication and characterization of single crystal FET transistors

Charge transport properties were measured using field-effect transistors fabricated on single crystals. We used graphite ink to paint source, drain and gate electrodes while a Parylene-N film served as gate dielectric[10,33,34]. Parylene-N was deposited on top of the crystal in a home-made reactor, and its thickness was determined with a profilometer. The channel capacitance was then calculated from the measured thickness and the tabulated dielectric constant of Parylene. The characteristics of the OFETs were measured using two Keithley 6517A electrometers under ambient conditions.

Results and discussion

The synthesis of DCP followed a previously published procedure for synthesizing tetrachlorotetracene,[10] as illustrated in scheme 1; this procedure is similar to that reported by Li et al.[25] However, in the second step, we used NaI as the reducing reagent instead of $SnCl_2$, which eliminated the necessity of using concentrated HCl and shortened the reaction time from 4 hours to 30 minutes. The product was a dark purple needle-shaped crystalline solid, isolated in a yield of 86%. The product doesn't have a clear melting point as reported in ref. 24, but sublimes when heated and decomposes above 330^{o}C in the air. Both NMR and Mass Spectrum confirm the formation of DCP.

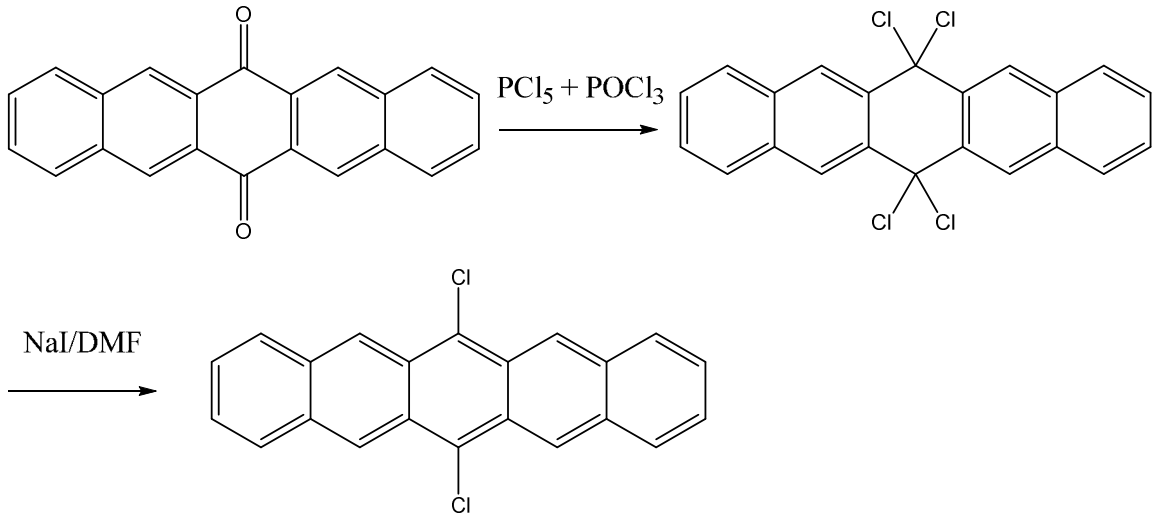

Scheme 1 The Synthetic procedures of 6,13-dichloropentacene.

DCP crystallizes as very thin needles by the physical vapor transport method; the crystals belong to $P2_1/c$ space group with a monoclinic unit cell. Table 1 shows a comparison of the crystal data of the two polymorphs.

Table 1. Crystal data of two polymorphs of 6,13-Dichloropentacene

	by PVT method	from solution[25]
Crystal system	monoclinic	monoclinic
Space group	$P2_1/c$	$P2_1/c$
Unit cell dimensions	a = 8.6812(9) Å b = 4.9972(6) Å c = 17.5379(18) Å β= 97.339(6)°	a = 3.8836(11) Å b = 18.718(5)Å c = 10.383(3) Å β= 94.058(5) °
Z	2	2
Cell volume	754.59	752.88

We also performed X-ray Powder Diffraction analysis of the PVT polymorph (see Supporting Information), but comparison of the diffraction pattern with an earlier publication of DCP[26] couldn't be made due to the low quality XRD spectrum.

The nearly planar molecular structure is illustrated in Figures 1a and b in different orientations.

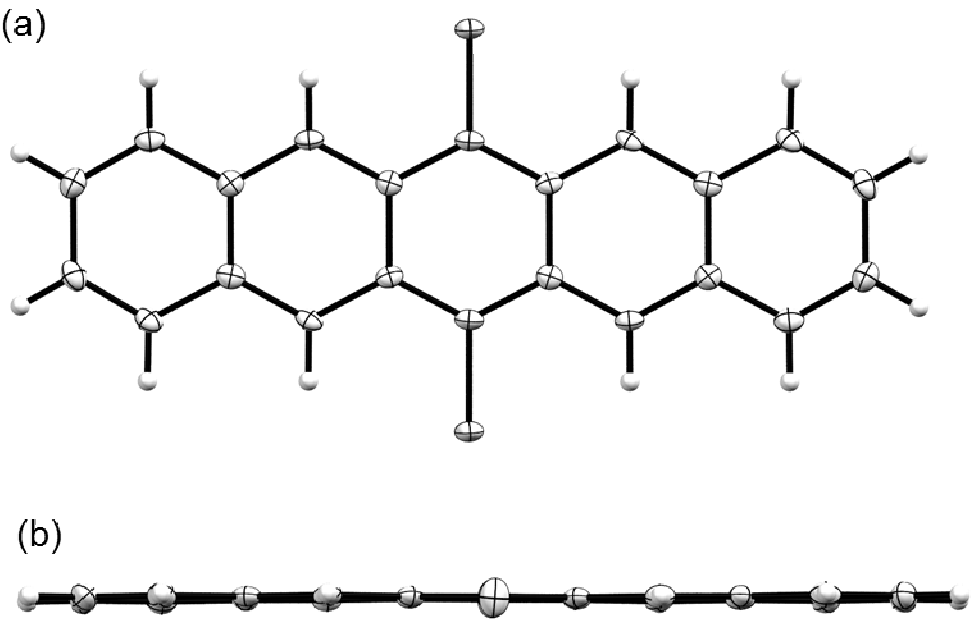

Figure 1. X-ray crystal structure of PVT grown DCP (a) view perpendicular to the molecular plan (b) view from the shorter edge.

The most important feature of molecular packing in both polymorphs is the stacking pattern (Figure 2a). Within each stack, both polymorphs show a similar displacement parallel to the short molecular axis (0.69 Å) compared to a perfectly cofacial stacking, which generates a graphitic registry between molecular planes (Figure 3) in which there are two kinds of carbon atoms: those that are approximately superimposed and those which lie above the centers of the benzene rings. The displacement along the long molecular axis, however, is quite different. As shown in Figure 3 the displacement in the PVT crystals is 3.6 Å (about one and a half times the length of a benzene ring), compared with a 1.2 Å displacement (half of the length of a benzene ring) found in the solution grown crystals. The large displacements in PVT crystals result in eight superimposed carbon atoms between neighboring molecules within a stack; whereas in solution grown crystals, ten carbon atoms are superimposed. The average interplanar distance in PVT crystals (3.39Å, Figure 2) is slightly shorter than that of solution grown crystals (3.47Å). Similar to solution grown polymorph, C–H···Cl interactions are also found in PVT crystals (Figure 3b).

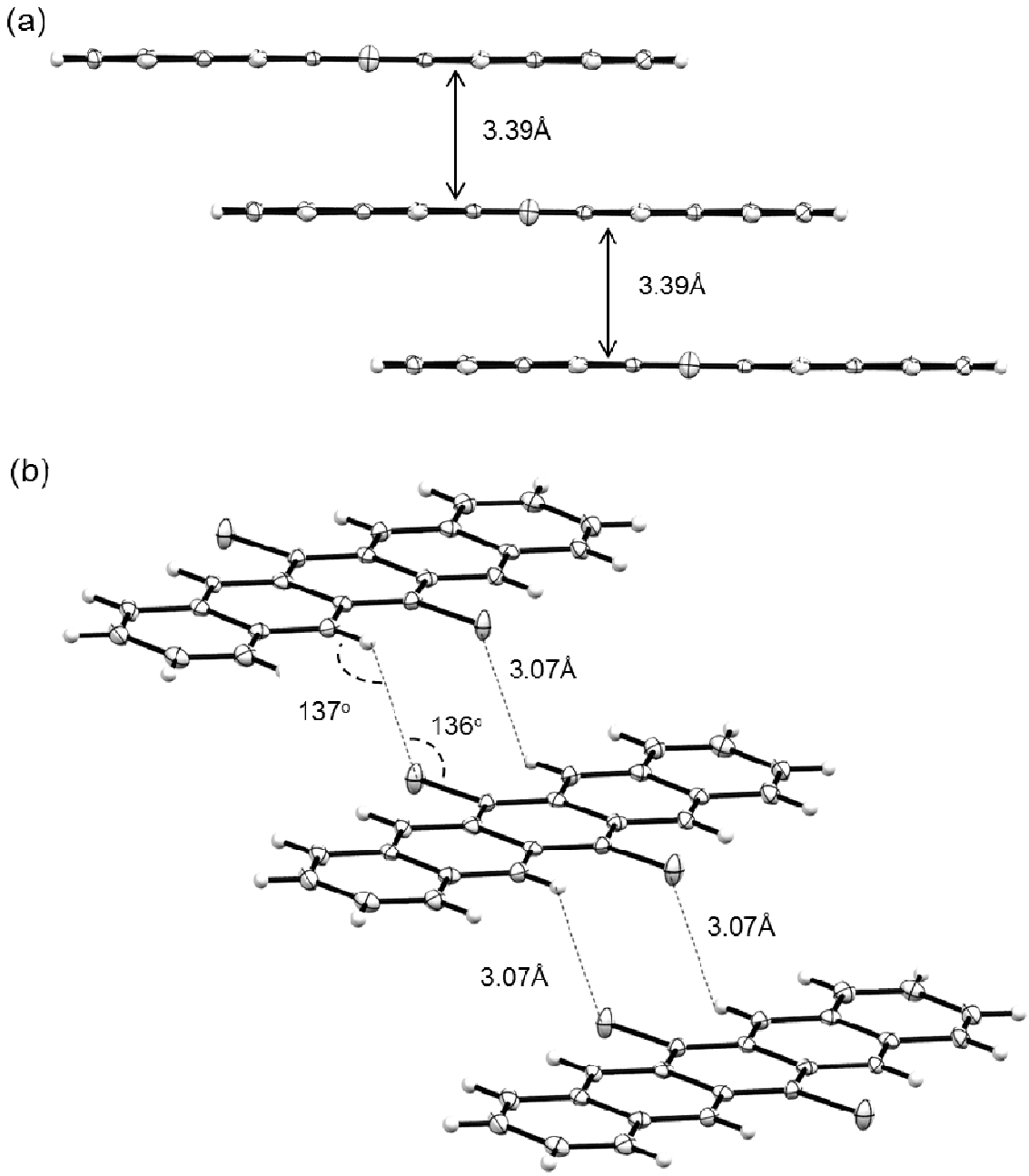

Figure 2 Packing structure of PVT grown DCP showing (a) stacking arrangement of DCP molecules and (b) C–H···Cl interactions between molecules of neighboring stacks.

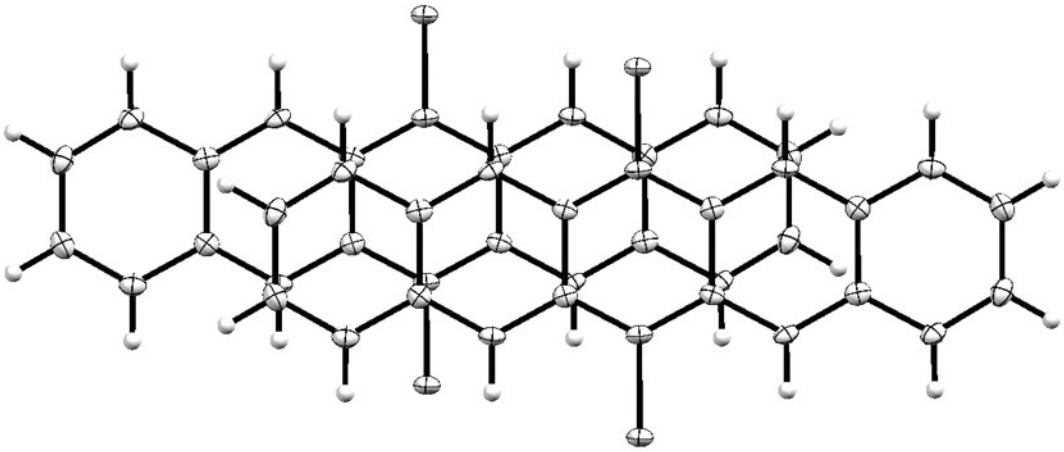

Figure 3 Two neighboring molecules overlap with 8 carbon atoms superimposed in the PVT polymorph. The closest carbon-carbon contact is 3.37Å.

Unconventional hydrogen-bonding interactions, such as C–H···X (X is an electronegative atom or anion, or π system, etc.), have recently been recognized as important stabilizing forces in crystal engineering.[35,36] These interactions, particularly when involving halogen atoms, are anisotropic.[37,38] In structures with C-H···Cl interactions, for example, the H···Cl distance is strongly angular dependent, which is more pronounced in compounds with chloride anions than neutral chloride-containing molecules.[39] While some C-H···Cl angles are close to linear ($\alpha_{C\text{-}H\cdots Cl}$ ~180) with H···Cl distance shorter than the sum of the van der Waals radii (2.95[40]), contacts outside the cutoff are also common with a well-defined angular dependence. It was therefore suggested that the conceptual van der Waals cut-off criterion should be replaced by a distance/angle criterion for establishing the presence of C-H···Cl interactions. [39]

In both PVT and solution grown crystals, the C-H···Cl angles are significantly smaller than 180° (137 ° and 128 °, respectively), and the H···Cl distance slightly larger than the sum of the van der Waals radii (3.07 Å and 3.13 Å, respectively). These angle-distance combinations fall within the range of the reported C-H···Cl interactions.[39] It appears that both polymorphas are stabilized by intrastacking π-π interaction, together with

interstacking C-H···Cl interactions. It is however unclear how the subtle differences in these interactions cause the formation of the two polymorphs.

Single crystal field-effect transistors were fabricated using graphite ink as electrodes and parylene as gate dielectric, and the transistor characteristics are illustrated in Figs. 4. A nonlinear dependence of the drain current on voltage V_{DS} is observed at low drain–source voltage, suggesting non-Ohmic contact behavior. At higher voltages, however, saturation is observed. From the transfer characteristics in Fig. 4b we extracted an on/off current ratio of 10^4, a threshold voltage of $V_t \sim -23$ V and a field-effect mobility of 0.43 cm^2/V s. This mobility is slightly higher than the values reported for the thin film and the solution grown microribbon DCP transistors.[25,26] The fairly large threshold voltage indicates a large trap density, which could be a significant factor in reducing the FET mobility. We performed single crystal field-effect transistor measurement on crystals of three different batches, with broad distribution of mobility: 0.07 cm^2/V s, 0.25 cm^2/V s and 0.43 cm^2/V s. The needle-shaped crystals are very thin and narrow, and the fabrication of the devices using these tiny crystals turned out to be difficult, which maybe the reason for the poor reproducibility. The broad distribution of mobility was also observed in other SC FET measurement.[41]

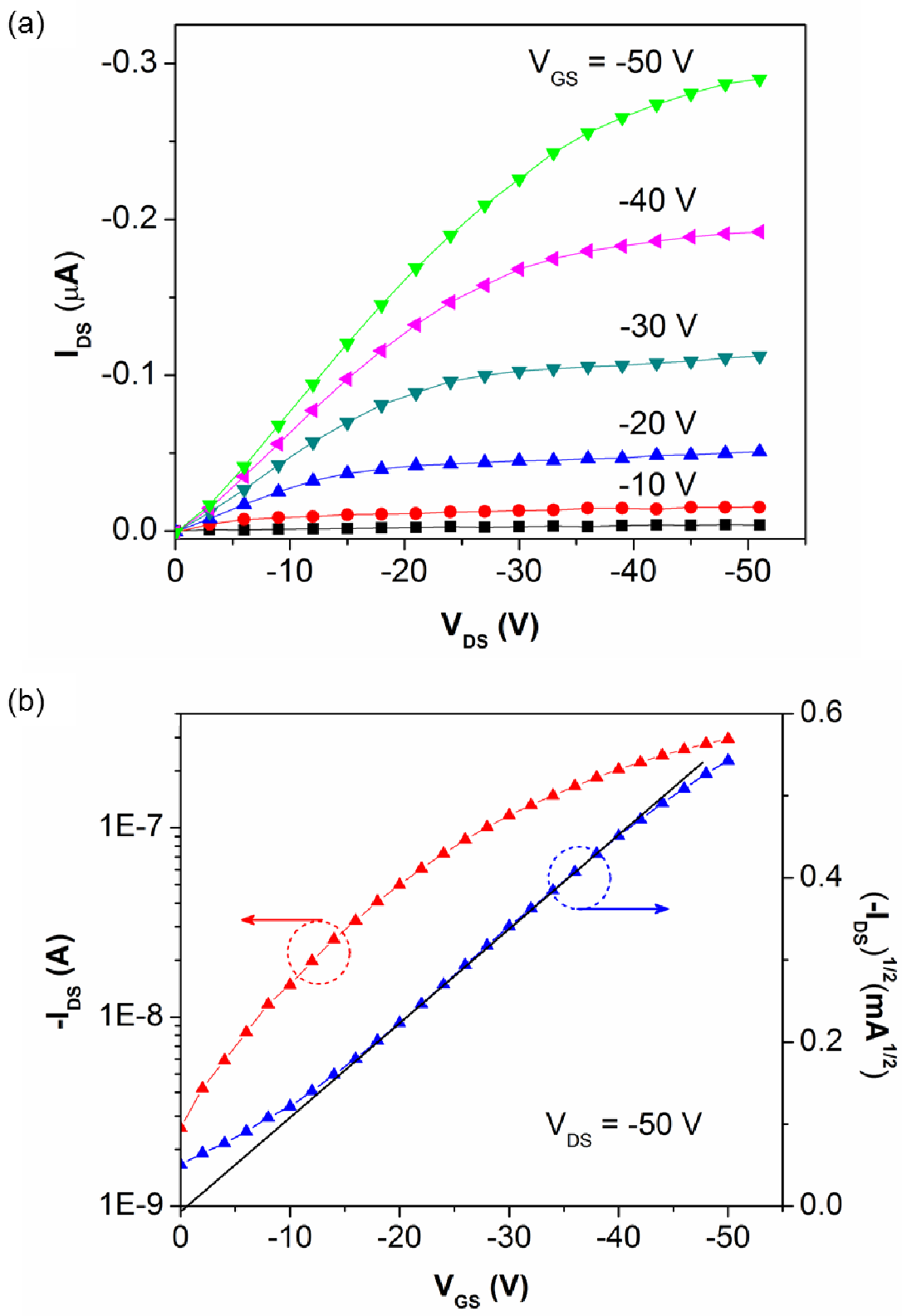

Figure 4 (a) Output and (b) transfer current-voltage characteristics of a single-crystal transistor based on 6,13-dichloropentacene (DCP) with channel dimension W/L = 0.2.

The π-stacking pattern, together with the short interplanar distance and the small intrastacking displacement, seems to be favorable for the mobility. However, the single crystal field effect transistor mobility measured here is only slightly better than those measured in DCP thin-films and the solution grown microribbons. The low performance could be attributed to the fact that the crystals were grown without any purification, and that the very thin and narrow needle shape of the crystals magnifies the surface effect. It is noteworthy that microribbons grown in the vapor phase were reported to show an average mobility of 5.71 cm^2/Vs in 14 independent devices, with the highest mobility reaching 9.0 $cm^2/V\ s$.[26]

Recently a number of new organic semiconductors have been synthesized and crystallized in π-stacking patterns, and the mobilities are generally anisotropic, with values of the order of 1 cm^2/Vs.[10,12,16,41,42] Among all the molecules with their various stacking patterns, however, rubrene still remains as the benchmark material, and its mobility can easily exceed 10cm^2/Vs. Theoretical calculations[6,43] show that transfer integrals along the stacking direction oscillate with the molecular displacements along the long molecular axis, which is maximal for the perfectly cofacial situation, and vanishes for large displacements. In Rubrene crystals, there is no short-axis displacement along the stacking direction and the displacement along the long molecular axis is 6.13 Å, about twice the value found in DCP. Interestingly, this large displacement in the rubrene crystal actually closely corresponds to extrema in the oscillations of both the HOMO and LUMO transfer integrals[43], which helps to explain the high mobility of rubrene crystals, even though there is a large long-axis displacement. Thus, the expectation that a short π-stacking distance, together with a small intermolecular displacement with a large number of superimposed carbon atoms will lead to a large band dispersion is not always correct, and quantum mechanical calculations are necessary to determine the intermolecular interactions.

We performed extended Huckel theory (EHT) calculations of the band electronic structures of both DCP polymorphs (Figure 5 and 6), as EHT band structure calculations

have been widely used in the rationalizations of the electronic structure of organic electronic materials.[8,9]The 1-D nature of the valence band (hole conduction) can be clearly seen from Figure 5 for PVT DCP, and the greatest dispersions are along the Y direction, in accordance with the stacking (along b): 0.25 eV in valence band and 0.31 eV in conduction band. In comparison, solution grown DCP also shows 1-D electronic structure (along X), but the dispersions are smaller, particularly in the valence band (0.1 eV, Figure 6). These results are in accord with the structure analysis: the interplanar distance in PVT polymorph is 3.39Å, smaller than that in solution grown crystal (3.47Å). Thus, the band structure calculation suggests that the PVT polymorph has stronger electronic coupling, and should have improved intrinsic charge-carrier properties relative to solution grown polymorph.

We also performed EHT band electronic structure calculation of rubrene as a comparison (Figure 7). The rubrene crystal displays significantly dispersion along Y in the valence band in addition to a large dispersion of 0.4 eV along X. A recent INDO calculation[43] on rubrene also reveals significant dispersion along the diagonal direction with the largest dispersion of 0.34 eV along the stacking direction. Thus, even though the interplanar distance and the intrastacking displacement are both smaller in PVT DCP than in rubrene crystals, the band width is larger in Rubrene. This calculation suggest that, if the electronic coupling is a dominant factor in determining the carrier mobility, both DCP polymorphs have lower intrinsic charge-carrier properties relative to rubrene, with the solution grown polymorph the lowest.

There are many factors that affect the carrier properties and a recent study[44] on rubrene and its derivatives shows that the charge carrier improvement in rubrene cannot be attribute to the rubrene endoperoxide formation in the presence of oxygen, and other processes favoring intermolecular electron transfer have to be found. McGarry and coworkers reported a series of new rubrene derivatives,[41] and their calculations indicate that the band dispersions in these crystals are comparable with, and in some cases even larger than in rubrene crystals. On the other hand, the measured mobilities are much less than expected (generally less than 1cm^2/Vs). Thus, there are other factors besides the band structure, such as the charge injection efficiency which need to be taken into account when accounting for the single-crystal mobility. In designing organic

semiconductors, however, it is still important to have molecules with large band dispersions (plus small reorganization energy) in order to realize high intrinsic mobility.

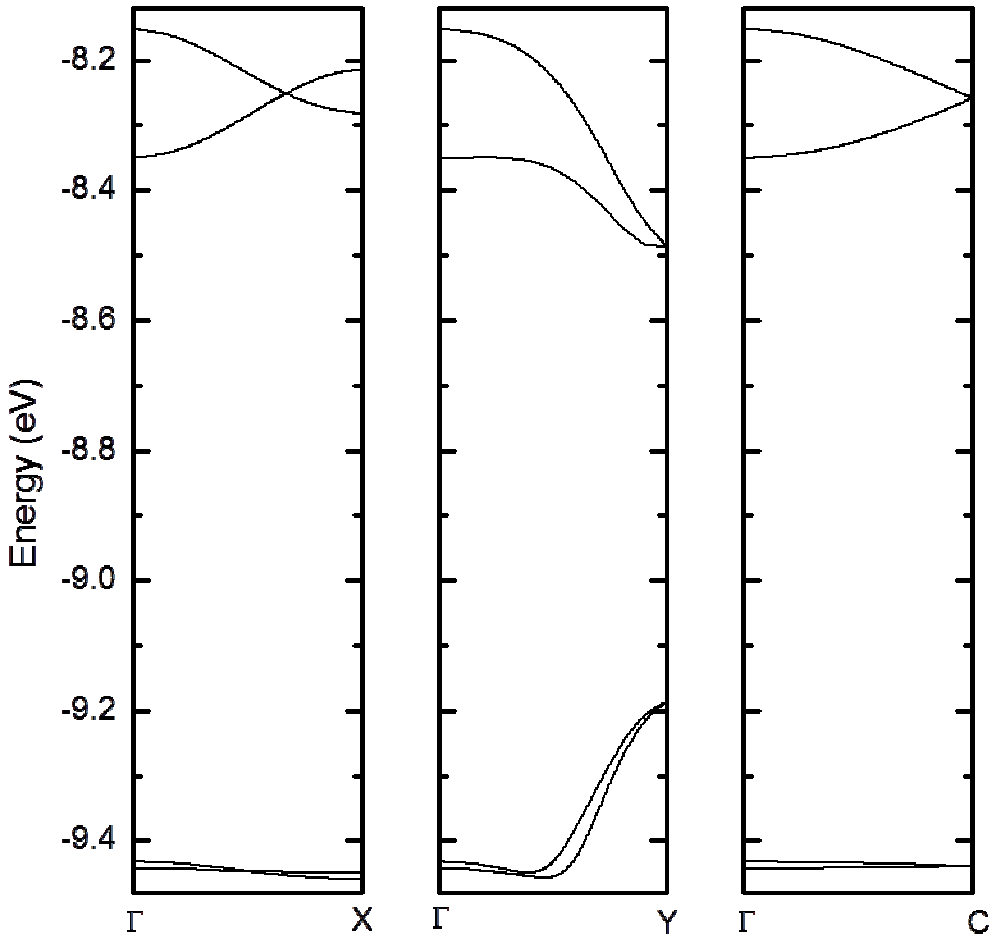

Figure 5 Electronic structure of the valence and conduction bands of PVT 6,13-dichloropentacene (DCP)

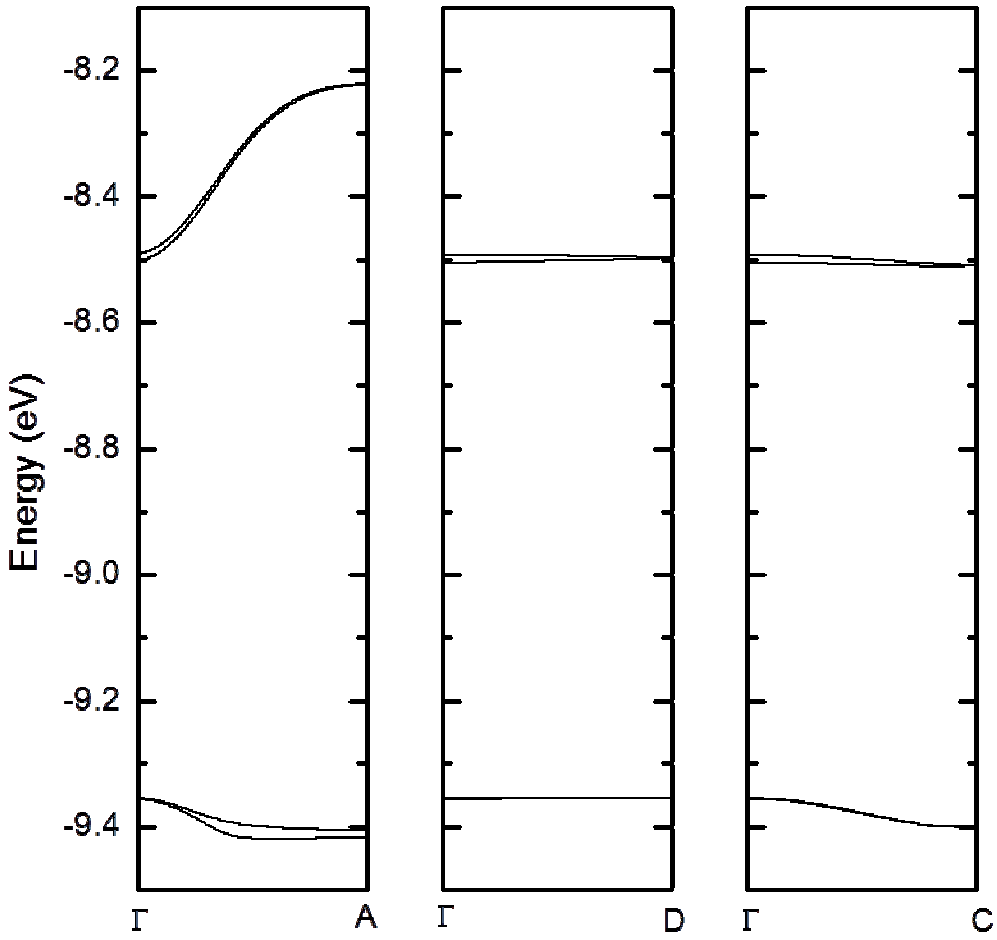

Figure 6 Electronic structure of the valence and conduction bands of solution grown crystals of 6,13-dichloropentacene (DCP)

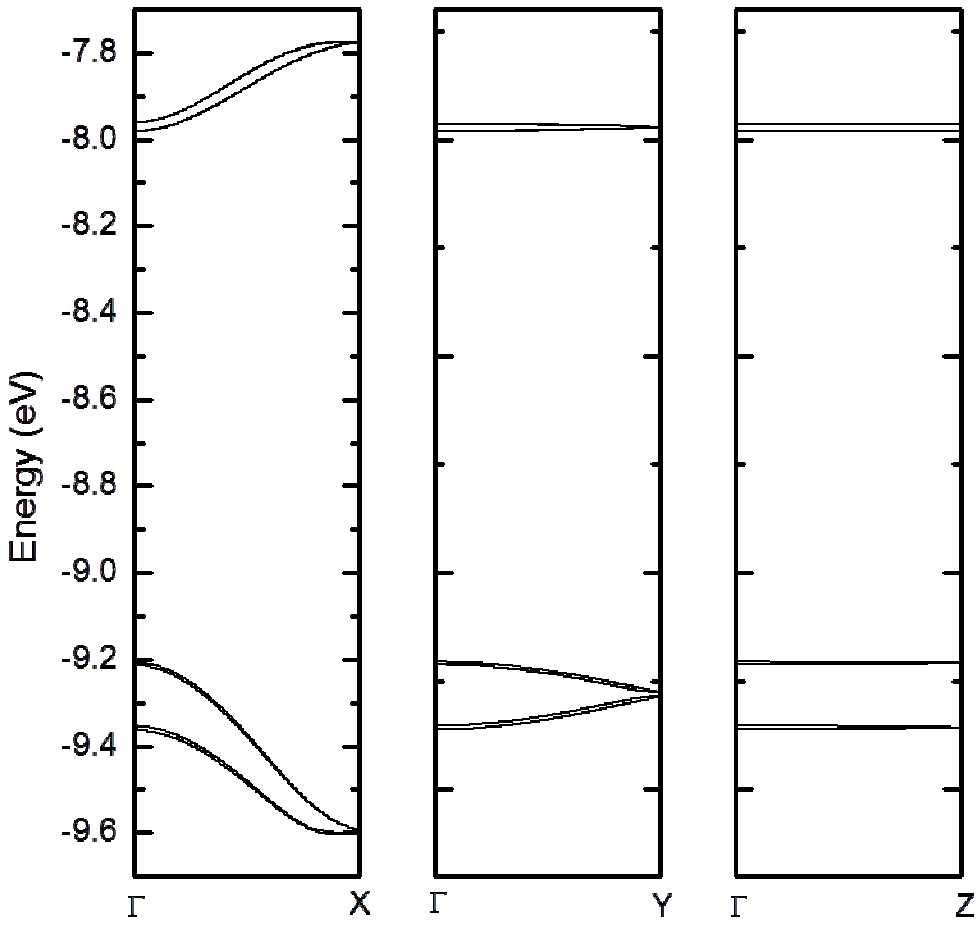

Figure 7 Electronic structure of the valence and conduction bands of Rubrene

Conclusion

We report the crystal structure of a DCP polymorph grown by the PVT method; this molecule crystalizes as very thin needles, and packs in a π-stacking pattern, with shorter interplanar distance and smaller intrastacking displacement compared with the solution grown polymorph. The field-effect mobility is on the order of 0.5 cm^2/Vs without device optimization. EHT calculation indicates a 1-D electronic structure in both DCP polymorphs, but the PVT polymorph has larger valence band dispersion along the stacking direction. A comparison with rubrene crystal suggests that the band dispersion

in PVT DCP is smaller than that of rubrene. The magnitude of the intrastacking displacement alone is not enough to predict the strength of electronic interaction; the relative locations of the HOMO/LUMO coefficients are the important feature. Although there are many factors affecting mobility, in order to design molecules with intrinsic high mobility, it is important to find molecules which form stacks and also display a suitable intrastack displacement that maximizes the band dispersion, as in rubrene crystals.

Acknowledgements

The authors thank the Robert A. Welch Foundation Grant AC-0006 to the Department of Chemistry at Texas A&M University-Kingsville for support of this work. This work was also supported by the U.S. Department of Education Title V - Promoting Postbaccalaureate Opportunities for Hispanic Americans Grant Award P031M105058, and at UC Riverside by the Division of Materials Science and Engineering, Office of Basic Energy Sciences of the U.S. Department of Energy under Award Number DE-FG02-04ER46138.

Reference

(1) Anthony, J. E. *Chem. Rev.* **2006**, *106*, 5028.

(2) Dimitrakopoulos, C. D.; Malenfant, P. R. L. *Adv. Mater.* **2002**, *14*, 99.

(3) Klauk, H. *Chem. Soc. Rev.* **2010**, *39*, 2643.

(4) Li, H.; Giri, G.; Tok, J. B. H.; Bao, Z. *MRS Bull.* **2013**, *38*, 34.

(5) Katz, H. E. *Chem. Mater.* **2004**, *16*, 4748.

(6) Coropceanu, V.; Cornil, J.; Da Silva Filho, D. A.; Olivier, Y.; Silbey, R.; Bredas, J.-L. *Chem. Rev.* **2007**, *107*, 926.

(7) Coropceanu, V.; Li, H.; Winget, P.; Zhu, L.; Bredas, J.-L. *Annu. Rev. Mater. Res.* **2013**, *43*, 63.

(8) Haddon, R. C.; Chi, X.; Itkis, M. E.; Anthony, J. E.; Eaton, D. L.; Siegrist, T.; Mattheus, C. C.; Palstra, T. T. M. *J. Phys. Chem. B* **2002**, *106*, 8288.

(9) Haddon, R. C.; Siegrist, T.; Fleming, R. M.; Bridenbaugh, P. M.; Laudise, R. A. *J. Mater. Chem.* **1995**, *5*, 1719.

(10) Chi, X.; Li, D.; Zhang, H.; Chen, Y.; Garcia, V.; Garcia, C.; Siegrist, T. *Org. Electron.* **2008**, *9*, 234.

(11) Watanabe, M.; Chao, T.-H.; Chien, C.-T.; Liu, S.-W.; Chang, Y. J.; Chen, K.-Y.; Chow, T. J. *Tetrahedron Lett.* **2012**, *53*, 2284.

(12) Yagodkin, E.; Xia, Y.; Kalihari, V.; Frisbie, C. D.; Douglas, C. J. *J. Phys. Chem. C* **2009**, *113*, 16544.

(13) Curtis, M. D.; Cao, J.; Kampf, J. W. *J. Am. Chem. Soc.* **2004**, *126*, 4318.

(14) Mas-Torrent, M.; Rovira, C. *Chem. Rev.* **2011**, *111*, 4833.

(15) Mas-Torrent, M.; Hadley, P.; Bromley, S. T.; Ribas, X.; Tarres, J.; Mas, M.; Molins, E.; Veciana, J.; Rovira, C. *J. Am. Chem. Soc.* **2004**, *126*, 8546.

(16) Moon, H.; Zeis, R.; Borkent, E.-J.; Besnard, C.; Lovinger, A. J.; Siegrist, T.; Kloc, C.; Bao, Z. *J. Am. Chem. Soc.* **2004**, *126*, 15322.

(17) Mattheus, C. C.; Dros, A. B.; Baas, J.; Oostergetel, G. T.; Meetsma, A.; de Boer, J. L.; Palstra, T. T. M. *Synth. Met.* **2003**, *138*, 475.

(18) Troisi, A.; Orlandi, G. *J. Phys. Chem. B* **2005**, *109*, 1849.

(19) Podzorov, V.; Menard, E.; Borissov, A.; Kiryukhin, V.; Rogers, J. A.; Gershenson, M. E. *Phys. Rev. Lett.* **2004**, *93*, 086602/1.

(20) Takeya, J.; Yamagishi, M.; Tominari, Y.; Hirahara, R.; Nakazawa, Y.; Nishikawa, T.; Kawase, T.; Shimoda, T.; Ogawa, S. *Appl. Phys. Lett.* **2007**, *90*, 102120/1.

(21) Huang, L.; Liao, Q.; Shi, Q.; Fu, H.; Ma, J.; Yao, J. *J. Mater. Chem.* **2010**, *20*, 159.

(22) Matsukawa, T.; Yoshimura, M.; Sasai, K.; Uchiyama, M.; Yamagishi, M.; Tominari, Y.; Takahashi, Y.; Takeya, J.; Kitaoka, Y.; Mori, Y.; Sasaki, T. *J. Cryst. Growth* **2010**, *312*, 310.

(23) Pfattner, R.; Mas-Torrent, M.; Bilotti, I.; Brillante, A.; Milita, S.; Liscio, F.; Biscarini, F.; Marszalek, T.; Ulanski, J.; Nosal, A.; Gazicki-Lipman, M.; Leufgen, M.; Schmidt, G.; Molenkamp, L. W.; Laukhin, V.; Veciana, J.; Rovira, C. *Adv. Mater.* **2010**, *22*, 4198.

(24) Giri, G.; Li, R.; Smilgies, D. M.; Li, E. Q.; Diao, Y.; Lenn, K. M.; Chiu, M.; Lin, D. W.; Allen, R.; Reinspach, J.; Mannsfeld, S. C.; Thoroddsen, S. T.; Clancy, P.; Bao, Z.; Amassian, A. *Nat. Commun.* **2014**, *5*, 3573.

(25) Li, J.; Wang, M.; Ren, S.; Gao, X.; Hong, W.; Li, H.; Zhu, D. *J. Mater. Chem.* **2012**, *22*, 10496.

(26) Wang, M.; Li, J.; Zhao, G.; Wu, Q.; Huang, Y.; Hu, W.; Gao, X.; Li, H.; Zhu, D. *Adv. Mater.* **2013**, *25*, 2229.

(27) Laudise, R. A.; Kloc, C.; Simpkins, P. G.; Siegrist, T. *J. Cryst. Growth* **1998**, *187*, 449.

(28) Dolomanov, O. V.; Bourhis, L. J.; Gildea, R. J.; Howard, J. A. K.; Puschmann, H. *J. Appl. Crystallogr.* **2009**, *42*, 339.

(29) Sheldrick, G. M. *Acta Crystallogr., Sect. A: Found. Adv.* **2015**, *71*, 3.

(30) Sheldrick, G. M. *Acta Crystallogr., Sect. A: Found. Crystallogr.* **2008**, *64*, 112.

(31) Andrews, M. P.; Cordes, A. W.; Douglass, D. C.; Fleming, R. M.; Glarum, S. H.; Haddon, R. C.; Marsh, P.; Oakley, R. T.; Palstra, T. T. M.; et, a. *J. Am. Chem. Soc.* **1991**, *113*, 3559.

(32) Cordes, A. W.; Haddon, R. C.; Oakley, R. T.; Schneemeyer, L. F.; Waszczak, J. V.; Young, K. M.; Zimmerman, N. M. *J. Am. Chem. Soc.* **1991**, *113*, 582.

(33) Butko, V. Y.; Chi, X.; Ramirez, A. P. *Solid State Commun.* **2003**, *128*, 431.

(34) Podzorov, V.; Pudalov, V. M.; Gershenson, M. E. *Appl. Phys. Lett.* **2003**, *82*, 1739.

(35) Sarma, J. A. R. P.; Desiraju, G. R. *Acc. Chem. Res.* **1986**, *19*, 222.

(36) Steiner, T. *Angew. Chem., Int. Ed.* **2002**, *41*, 48.

(37) Day, G. M.; Price, S. L. *J. Am. Chem. Soc.* **2003**, *125*, 16434.

(38) Price, S. L.; Stone, A. J.; Lucas, J.; Rowland, R. S.; Thornley, A. E. *J. Am. Chem. Soc.* **1994**, *116*, 4910.

(39) Aakeroy, C. B.; Evans, T. A.; Seddon, K. R.; Palinko, I. *New J. Chem.* **1999**, *23*, 145.

(40) Bondi, A. *J. Phys. Chem.* **1964**, *68*, 441.

(41) McGarry, K. A.; Xie, W.; Sutton, C.; Risko, C.; Wu, Y.; Young, V. G., Jr.; Bredas, J.-L.; Frisbie, C. D.; Douglas, C. J. *Chem. Mater.* **2013**, *25*, 2254.

(42) Mamada, M.; Katagiri, H.; Sakanoue, T.; Tokito, S. *Cryst. Growth Des.* **2015**, *15*, 442.

(43) da Silva Filho, D. A.; Kim, E.-G.; Bredas, J.-L. *Adv. Mater.* **2005**, *17*, 1072.

(44) Uttiya, S.; Miozzo, L.; Fumagalli, E. M.; Bergantin, S.; Ruffo, R.; Parravicini, M.; Papagni, A.; Moret, M.; Sassella, A. *J. Mater. Chem. C* **2014**, *2*, 4147.

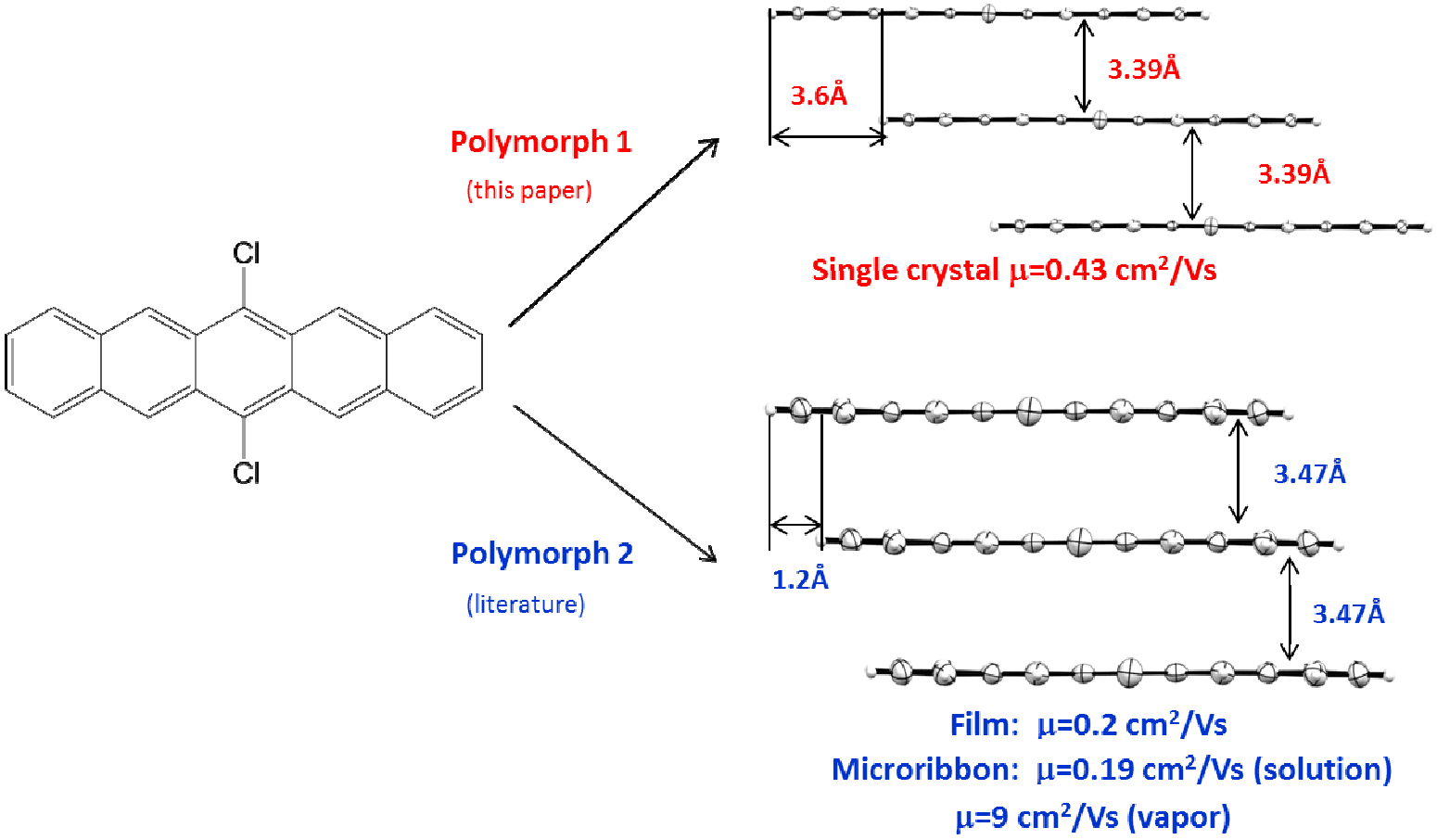

A new polymorph of 6,13-dichloropentacene organic semiconductor was discovered, and its properties were compared with those of an earlier reported polymorph.

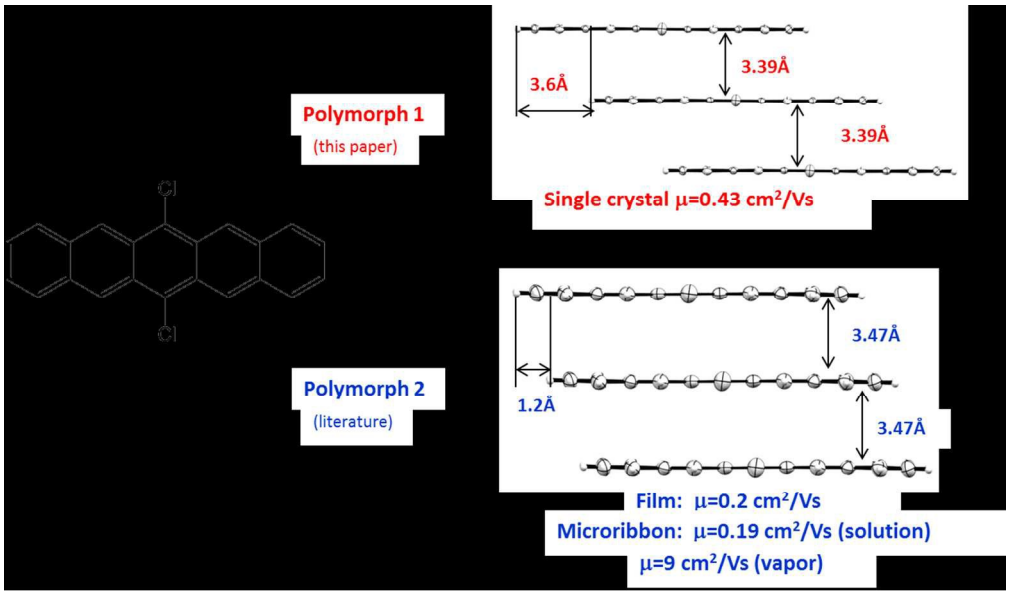

214x125mm (150 x 150 DPI)